Novel route to synthesize CuO nanoplatelets

R.A. Zarate[a],*, F. Hevia[b], S. Fuentes[a], V.M. Fuenzalida[c], A. Zúñiga[d]

[a]*Departamento de Física, Facultad de Ciencias, Universidad Católica del Norte, Casilla 1280, Antofagasta, Chile*
[b]*Departamento de Química, Facultad de Ciencias, Universidad Católica del Norte, Casilla 1280, Antofagasta, Chile*
[c]*Departamento de Física, Facultad de Ciencias Físicas y Matemáticas, Universidad de Chile, Av. Blanco Encalada 2008, Santiago, Chile*
[d]*Departamento de Ingeniería Mecánica, Facultad de Ciencias Físicas y Matemáticas, Universidad de Chile, Beauchef 850, Santiago, Chile*

Abstract

A new synthesis route to obtain high-purity cupric oxide, CuO, using the hydrothermal reaction of copper sulfide and a NaOH solution in an oxygen atmosphere has been developed. The synthesized products showed nanoplatelet-like morphologies with rectangular cross-sections and dimensions at the nanometric scale. Variations in the oxygen partial pressure and synthesis temperature produced changes in size and shape, being found that the proliferation of nanoplatelet structures occurred at 200 °C and 30 bar.
© 2007 Published by Elsevier Inc.

1. Introduction

In recent years, the synthesis and production of one-dimensional (1D) materials has received much attention due to their excellent physical and chemical properties in comparison to their bulk counterparts, and their potential applications in nanocomposite materials and nanoscale devices as interconnectors for nanoelectronics [1–6].

Among the materials based on 3*d* transition metals, cupric oxide (CuO) is of great interest due to its properties such as catalytic and as well as its close connection to high-temperature superconductors [7,8]. CuO is a p-type semiconductor with a band gap of 1.2 eV, and since this gap is smaller than 1.85 eV, this compound has started to be studied for its field emission properties [9]. Moreover, CuO has interesting photovoltaic, electrochemical and catalytic properties [10–13]. On the other hand, the large fraction of surface area, excellent stability, low production cost, and good electric properties of nanostructured CuO have fueled new studies to determine its applicability as material for solar cells, in particular due to its photo-conductivity and photochemical properties.

On the other hand, a number of different techniques have been used to fabricate nanostructured CuO, such as heating of copper sheets in an O_2 atmosphere [14]. Similarly, CuO nanorods have been prepared by direct reaction with ammonia solutions [15], electrodeposition of Cu(II) ions followed by gas–solid reaction [16], or using a wet chemical route involving NaOH and Cu^{2+} [17]. The typical route used by several investigators has been the use of $Cu(OH)_2$ with tape-like structure, or wire as insoles [18–20]. CuO nanorod and nanoribbons have been also synthesized at moderate temperatures (77–85 °C) in a water–ethanol solution [21]. Among these various synthesis methods, hydrothermal or chemical reaction methods are of great interest because they are safe and environment-friendly synthesis procedures performed at moderate temperatures (around 200 °C).

In this work, we inform of a new route to directly synthesize highly crystalline CuO nanoplatelets via the hydrothermal reaction of copper sulfide and a NaOH solution in an oxygen atmosphere. This investigation represents the first step towards producing pure crystalline CuO at a large scale with morphology control.

---

*Corresponding author. Fax: +56 55 355521.
  E-mail address: rzarate@ucn.cl (R.A. Zarate).

2. Experimental section

The material was produced by dissolving 5.0 g of Cu_xS into 40 mL of NaOH solution (10 M) under continuous stirring until a homogeneous solution was formed. The mixed solution was transferred into a 100 mL Teflon-lined stainless steel reactor, sealed, and then heated at three different temperatures (150, 200 and 230 °C) for 90 min under two different oxygen partial pressures (10 or 30 bar). At the end of the reaction, the autoclave was naturally cooled to room temperature. The black powder that was attached to the bottom and inner wall of the Teflon container was collected, centrifuged, washed with distilled water and ethanol to remove the remaining ions, and dried at 60 °C for 6 h in vacuum.

The black powder was characterized by X-ray diffraction (XRD) using a Siemens D 5000 diffractometer with CuKα radiation (40 kV, 30 mA). X-ray photoelectron spectroscopy (XPS) was carried out using a Physical Electronics Model 1257 system. The XPS peaks were calibrated using the C 1s line at 284.5 eV.

The morphology of the samples was examined using a low-vacuum scanning electron microscope (LV-SEM, JSM-5900LV) equipped with an EDX detector, and a field emission scanning electron microscope (FEG-SEM JSM-6330F) equipped with a digital acquisition system. Transmission electron microscopy (TEM) studies were performed in a Tencai F20 FEG-TEM operated at 200 kV equipped with an EDS detector. The TEM samples were prepared by suspending the powder in ethanol and then collecting it using a carbon grid.

3. Results and discussion

3.1. Structural analysis

XRD analyses were used to study the phases present in the hydrothermal samples, as shown in Fig. 1. The XRD pattern in Fig. 1a corresponds to the precursor, which clearly indicates the presence of covallite (CuS) and digenite (Cu_9S_5) with small quantities of chalcocite (Cu_2S).

On the other hand, the XRD patterns of samples treated at 150/10 (°C/bar) exhibited two crystalline phases (Fig. 1b), CuO and CuS (JCPDS cards no. 48-1548 and 06-0464, respectively). The low temperature and oxygen partial pressure did not allow the consumption of the entire precursor, suggesting a gradual transformation of the starting material (CuS) into CuO.

Figs. 1c and d show XRD patterns of samples that were treated at 150/30 and 200/30 (°C/bar), respectively. All the peaks can be clearly indexed as monoclinic CuO (space group $C2/c$), and the calculated lattice constants are in good agreement with the tabulated values ($a = 4.684$ Å, $b = 3.425$ Å, $c = 5.129$ Å and $\beta = 99.47$ Å). Diffraction peaks corresponding to impurities such as CuS, $Cu(OH)_2$ or Cu_2O were not observed, suggesting that the CuO product is a pure crystalline phase. The major peaks
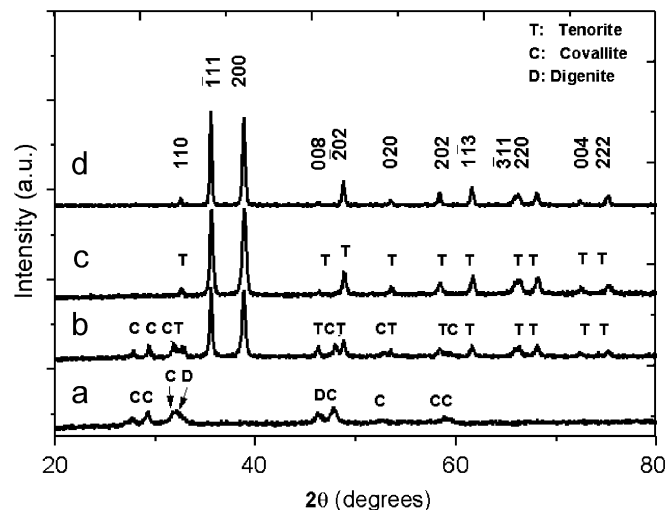

Fig. 1. XRD patterns of the precursor (graph (a)) and CuO nanoplatelets obtained by hydrothermal reaction under different synthesis conditions: (b) 150/10, (c) 150/30 and (d) 230/10 (°C/bar). The reaction time used in all samples was 90 min.

located at 2θ values between 30° and 65° (35.5°, 38.7°, 48.8° and 58.4°) can be attributed to the Miller indexes of the (−1 1 1), (2 0 0), (−2 0 2) and (2 0 2) planes of monoclinic CuO, respectively.

3.2. Compositional analysis

The elemental composition and oxidation states of the samples were analyzed by X-ray photoelectron spectroscopy, and a typical survey XPS spectrum of the nanoplatelets is shown in Fig. 2a. The peaks located at 933.6 and 953.5 eV are attributed to Cu $2p_{3/2}$ and Cu $2p_{1/2}$, respectively, and those located at 941.7, 944.0 and 962.1 eV are attributed to the shake up lines (see top inset in Fig. 2a: a typical high-resolution XPS spectrum), which are indicatives of the Cu(II) oxidation state [21]. In order to confirm whether the Cu 2p line corresponds to only one oxidation state, the first peak of this line was fitted to only one Gaussian in several samples analyzed.

As shown in Fig. 2b, the O 1s core-level spectrum is broad, and three Gaussians (marked as I, II and III) were resolved by using a curve-fitting procedure. Peak I, at the lower energy of 529.8, is in agreement with that for O^{2-} in CuO [22]. Peaks II and III, at higher energies of 531.7 and 533.0 eV, are associated to OH groups and to water absorbed onto the surface of the CuO nanoplatelets, respectively. No other lines corresponding to impurities such as S 2p or Na 1s were detected, indicating the high purity of the as-obtained samples. Thus, the XPS results indicate that the samples are composed only of CuO.

Energy dispersive X-ray spectroscopy (EDX/SEM) analyses indicated that the sample prepared at low temperature and low oxygen partial pressure was composed of Cu, S and O (Fig. 3a). When the temperature or oxygen partial pressure was increased, the EDX spectra
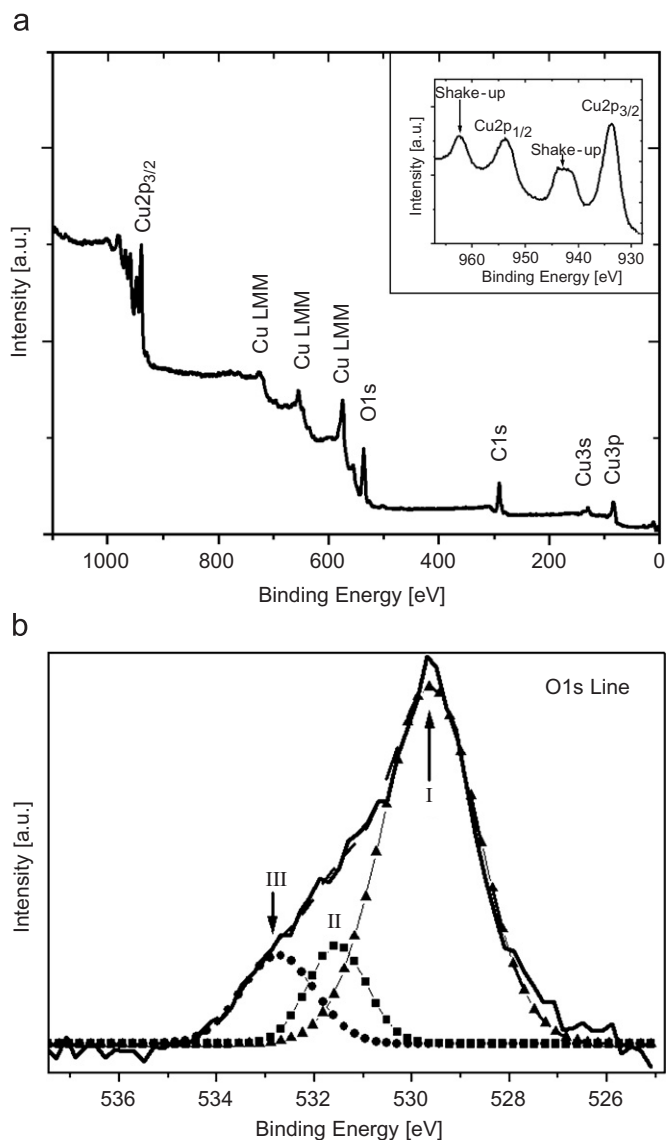
a

b

Fig. 2. XPS spectra of the CuO nanoplatelets prepared hydrothermally. Graph (a) is a typical XPS survey, the top inset is the typical high-resolution XPS spectrum in the Cu 2p line, and graph (b) O 1s line of nanoplatelets.

Fig. 3. EDX spectra of the CuO synthesized at (a) 150/10 and (b) 230/10 (°C/bar).
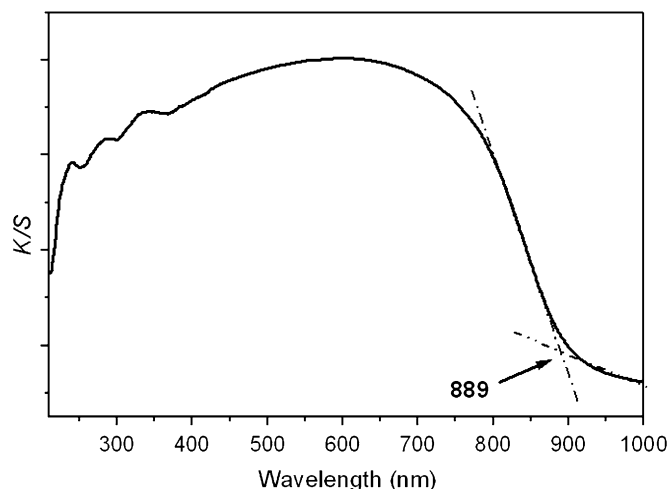
Fig. 4. UV–vis range diffuse reflectance of the CuO nanoplatelets of a sample prepared at 230/10 (°C/bar).

exhibited only Cu and O, while S was not detected (Fig. 3b). These spectra show the Cu$K\alpha$, $K\beta$ and L peaks at 8.055, 8.89 and 0.94 keV, respectively. The O $K\alpha$ peak is observed at 0.520 keV while a small aluminum peak is located at 1.48 keV. The chemical composition of the nanoplatelets was approximately 48 at% O and 52 at% Cu.

3.3. Optical properties

Diffuse reflectance measurements in the UV–vis range were carried out in order to obtain information on the electronic structure of the CuO nanoplatelets. A typical reflectance spectrum corresponding to nanoplatelets prepared at 230/10 (°C/bar) is shown in Fig. 4. The wavelength onset was estimated to be around 894 nm, i.e., the reflectance spectrum shows a strong absorption above
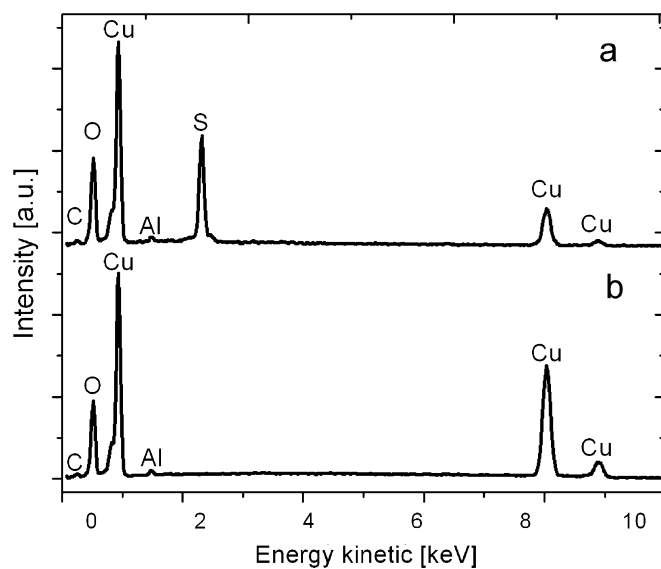
889 nm which corresponds to a band gap of 1.4 eV. This result suggests that this product can be used as high-performance solar cell [23]. The same results were obtained in a sample prepared at 150/30 (°C/bar), which also suffered a complete phase transformation from CuS to CuO.

3.4. Scanning electron microscopy and transmission electron microscopy

Hydrothermal treatments greatly influenced the morphology of the cupric oxide nanoplatelets. The morphological features of the nanoplatelets are highly dependent upon the temperature and the oxygen partial pressure in the autoclave during synthesis. In order to understand the growth process of the CuO nanoplatelets, samples

obtained at different stages of reaction were analyzed by FEG-SEM.

Figs. 5a and b show SEM images of samples obtained after hydrothermal reaction at 150/10 and 150/30 (°C/bar), respectively. When the oxygen partial pressure was 10 bar, the platelets have dimensions of ca. 0.7–1.0 μm in width and 1–3 μm in length, as shown in Fig. 5a. In contrast, at 30 bar there is a slight decrease in size of the platelets, which have widths of ca. 200–400 nm and lengths of ca. 0.6–1 μm. Another important characteristic is that under these conditions several nucleation sites were observed, in such a way that the growth of the cupric oxide can be seen as that of a flower. These fine nanoplatelets tend to aggregate in spindle-like bundles because of their high surface energy or van der Waals forces, similar to the bundles observed in carbon nanotubes [24].

However, when the temperature was increased from 150 to 230 °C while keeping the oxygen partial pressure constant at a value of 10 bar, the morphology changed completely to well-defined nanoplatelets (Fig. 5c), with dimensions of 400 nm–2 μm in width and lengths of 1 μm to several micrometers. These structures exhibit morphological defects which are possibly due to internal stresses developed during the synthesis. On the other hand, when the oxygen partial pressure was increased to 30 bar while keeping the temperature constant at 230 °C, the morphology was similar to that observed in Fig. 5b, where the nanoplatelets present an increase in size and a flower-like shape (Fig. 5d).

For an oxygen partial pressure of 30 bar and a temperature of 200 °C, we found that the samples exhibited important changes in morphology. Specifically, we observed the presence of many wire-like structures but with rectangular cross-section, i.e., wires with dimensions that
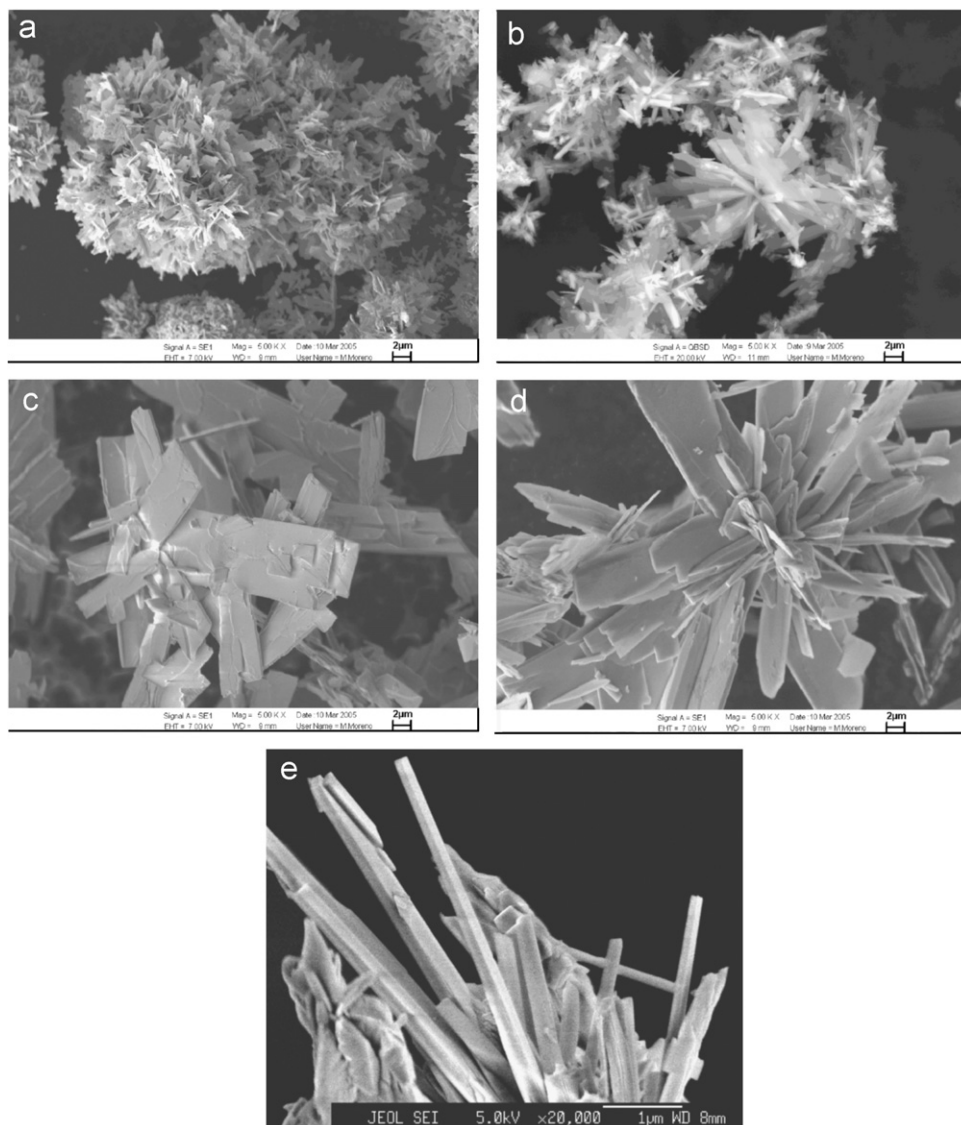

Fig. 5. SEM images of CuO hydrothermally treated samples at (a) 150/10, (b) 150/30, (c) 230/10, (d) 230/30 and (e) 200/30 (°C/bar); treatments were of 90 min.

varied from 100 up to 500 nm in width and 400 nm up to several micrometers in length, as can be seen in the SEM image of Fig. 5e.

The morphology and atomic structure of the nanoplatelets was further studied using TEM and HRTEM. Fig. 6 shows the morphology and internal structure of the CuO nanoplatelets. It can be observed that the nanoplatelets are for the most part monocrystalline (Fig. 6a), although the presence of crystal defects, such as twins was also detected (Fig. 6b). As discussed previously, these crystal defects may have formed during synthesis due to internal stresses. High-resolution images were taken to confirm the monoclinic structure of the CuO nanoplatelets, as shown in Fig. 7. Energy dispersive X-ray spectroscopy analyses of the CuO gave similar results to those obtained in the SEM, i.e., 48.5 at% O and 51.5 at% Cu.

These results suggest that the morphology of the CuO nanoplatelets can be modified by varying the reaction temperature or the oxygen partial pressure. We also determined the minimum values of temperature and oxygen partial pressure necessary to obtain a pure CuO phase.

The chemical reactions that are involved in the entire synthesis can be summarized as follows:

$$2CuS + 4O_2 + 4NaOH \rightarrow 2Cu(OH)_2 + 2Na_2SO_4, \qquad (1)$$

$$Cu(OH)_2 \rightarrow CuO + H_2O. \qquad (2)$$

There are a number of roles that the NaOH (helped by the O_2) played during the synthesis. The NaOH reacted with CuS to form $Cu(OH)_2$, which is then decomposed into CuO and water. Under our synthesis condition, the solution used was much more basic, so that the $Cu(OH)_2$ was unstable and the intermediate compound was not observed. Therefore, the alkaline media in addition to the temperature accelerated the decomposition of $Cu(OH)_2$ into CuO.

4. Conclusions

In summary, a simple hydrothermal route has been developed to obtain nanoplatelets and wires of CuO of high crystallinity through the reaction of CuS in a NaOH solution. The purity, morphology, particle size and crystallinity of the CuO powders varied with the synthesis parameters, such as reaction time, temperature, and oxygen partial pressure.

The samples that were treated at low temperature (150 °C) and low oxygen partial pressure (10 bar) exhibited the presence of both cupric oxide and copper sulfide. When the oxygen partial pressure was increased to 30 bar or the temperature was increased to 230 °C, the crystalline
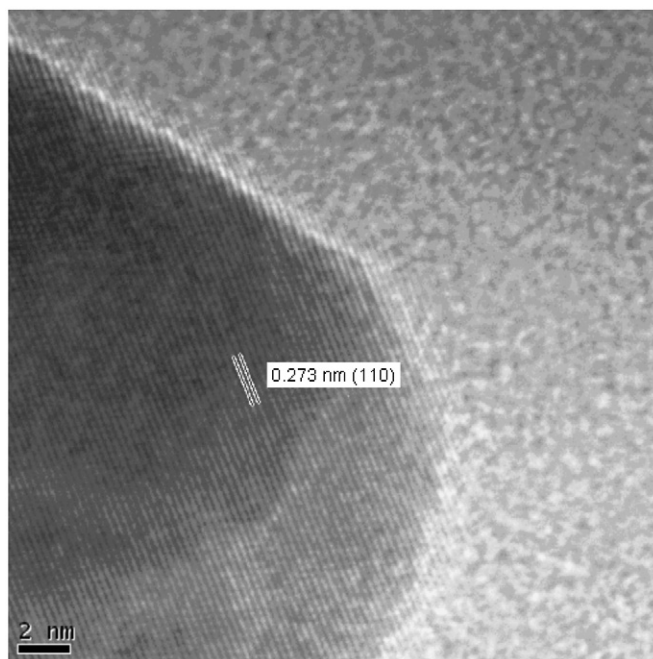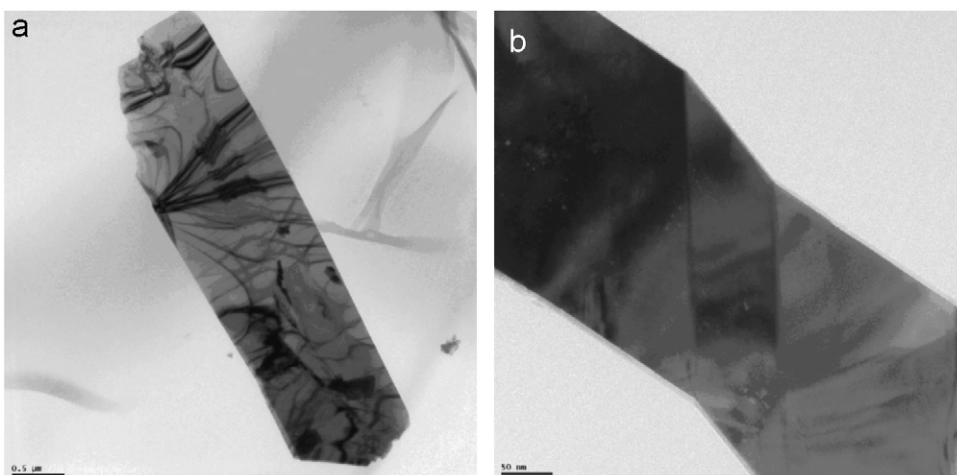

Fig. 7. HRTEM image of the CuO nanoplatelet.

Fig. 6. (a) BF TEM micrograph showing a single-crystal CuO nanoplatelet, and (b) BF TEM micrograph showing a twined crystal.

transformation from copper sulfide to cupric oxide was complete. Also, we found that the shape and size of the synthesized structures are controlled mainly by the oxygen partial pressure, the proliferation of nanoplatelet structures occurred at 200/30 (°C/bar). But the underlying growth mechanisms are not clear yet.

The synthesis of these nanocrystalline CuO powders avoids the use of any complex agent and does not require an elaborated pH control or expensive equipment. The route utilized makes it possible to produce highly pure materials at greatly reduced production costs, thus offering great opportunities for the scale-up manufacturing of semiconductor nanostructured materials.

Acknowledgments

References

[1] C.N. Rao, G. Kulkarni, P. Thomas, P. Edwards, Chem. Eur. J. 8 (2002) 29.
[2] W. Wang, I. Germanenko, M. El-Shall, Chem. Mater. 14 (2002) 3028.
[3] X. Zheng, C. Xu, Y. Tomokiyo, E. Tanaka, H. Yamada, Phys. Rev. Lett. 85 (2000) 5170.
[4] S. Yu, H. Colfen, M. Antonietti, Adv. Mater. 15 (2003) 133.
[5] Y. Xia, P. Yang, Y. Sun, Y. Wu, B. Meyers, B. Gates, Y. Yin, F. Kim, H. Yan, Adv. Mater. 15 (2003) 353.
[6] W. Fujita, K. Awaga, J. Am. Chem. Soc. 119 (1997) 4563.
[7] X. Song, S. Sun, W. Zhang, H. Yu, W. Fan, J. Phys. Chem. B 108 (2004) 5200.
[8] W. Wang, O. Varghese, C. Ruan, M. Paulose, C. Grimes, J. Mater. Res. 18 (12) (2003) 2756.
[9] M. Norman, A. Freeman, J. Phys. Rev. B 33 (1986) 8896.
[10] P. Podhajecky, Z. Zabransky, P. Novak, Z. Dobiasova, R. Cerny, V. Valvota, Electrochim. Acta 35 (1990) 245.
[11] M. Hara, T. Kondo, M. Cómoda, S. Ikeda, K. Shinohara, A. Tanaka, J. Kondo, K. Domen, Chem. Commun. (1998) 357.
[12] S. Nakayama, A. Kimura, M. Shibata, S. Kuwabata, T. Osakai, J. Electrochem. Soc. 148 (2001) 467.
[13] K. Nagase, Y. Zhang, Y. Kodama, J. Kakuta, J. Catal. 187 (1999) 123.
[14] X. Jiang, T. Herricks, Y. Xia, Nano Lett. 2 (12) (2002) 1333.
[15] L. Sun, Z. Zhang, Z. Wang, Z. Wu, H. Dang, Mater. Res. Bull., in press.
[16] B. Balamurugan, B. Mehta, S. Shivaprasad, Appl. Phys. Lett. 79 (2001) 3176.
[17] S. Anandan, X. Wen, S. Yang, Mater. Chem. Phys., in press.
[18] W. Wang, G. Wang, X. Wang, R. Zhan, Y. Liu, C. Zheng, Adv. Mater. 14 (2002) 67.
[19] X. Wen, W. Zhang, S. Yang, Langmuir 19 (2003) 5898.
[20] X. Wen, W. Zhang, S. Yang, Z.R. Dai, Z.L. Wang, Nano Lett. 2 (2) (2002) 1397.
[21] J. Moulder, W. Sticke, P. Sobol, K. Bomben, in: J. Chastain (Ed.), Handbook of X-ray Photoelectron Spectroscopy, Perkin Elmer Coorporation, Physical Electronics Division, USA, 1992.
[22] J. Xu, W. Ji, Z. Shen, S. Tang, X. Ye, J. Solid State Chem. 147 (1999) 516.
[23] S. Anandan, X. Wen, S. Yang, Mater. Chem. Phys. 93 (2005) 35.
[24] Y. Saito, Y. Tani, N. Miyagawa, K. Mitsushima, Chem. Phys. Lett. 294 (1998) 593.